frontiers | Frontiers in Astronomy and Space Sciences

TYPE Perspective
PUBLISHED 05 August 2024
DOI 10.3389/fspas.2024.1430099

OPEN ACCESS

EDITED BY
Yoshizumi Miyoshi,
Nagoya University, Japan

REVIEWED BY
Jean-Francois Ripoll,
CEA DAM Île-de-France, France

*CORRESPONDENCE
Martin O. Archer,
m.archer10@imperial.ac.uk

RECEIVED 09 May 2024
ACCEPTED 22 July 2024
PUBLISHED 05 August 2024

CITATION
Archer MO, Shi X, Walach M-T, Hartinger MD, Gillies DM, Di Matteo S, Staples F and Nykyri K (2024), Crucial future observations and directions for unveiling magnetopause dynamics and their geospace impacts. *Front. Astron. Space Sci.* 11:1430099. doi: 10.3389/fspas.2024.1430099

Crucial future observations and directions for unveiling magnetopause dynamics and their geospace impacts

Martin O. Archer[1]*, Xueling Shi[2,3], Maria-Theresia Walach[4], Michael D. Hartinger[5,6], D. Megan Gillies[7,8], Simone Di Matteo[9,10], Frances Staples[11] and Katariina Nykyri[10]

[1]Department of Physics, Imperial College London, London, United Kingdom, [2]Department of Electrical and Computer Engineering, Virginia Tech, Blacksburg, VA, United States, [3]High Altitude Observatory, National Center for Atmospheric Research, Boulder, CO, United States, [4]Physics Department, Lancaster University, Lancaster, United Kingdom, [5]Space Science Institute, Boulder, CO, United States, [6]Department of Earth, Planetary, and Space Sciences, University of California Los Angeles, Los Angeles, CA, United States, [7]Department of Physics and Astronomy, University of Calgary, Calgary, AB, Canada, [8]Department of Chemistry and Physics, Mount Royal University, Calgary, AB, Canada, [9]Physics Department, The Catholic University of America, Washington, DC, United States, [10]NASA-Goddard Space Flight Center, Greenbelt, MD, United States, [11]Department of Atmospheric and Oceanic Sciences, University of California Los Angeles, Los Angeles, CA, United States

The dynamics of Earth's magnetopause, driven by several different external/internal physical processes, plays a major role in the geospace energy budget. Given magnetopause motion couples across many space plasma regions, numerous forms of observations may provide valuable information in understanding these dynamics and their impacts. *In-situ* multi-point spacecraft measurements measure the local plasma environment, dynamics and processes; with upcoming swarms providing the possibility of improved spatiotemporal reconstruction of dynamical phenomena, and multi-mission conjunctions advancing understanding of the "mesoscale" coupling across the geospace "system of systems." Soft X-ray imaging of the magnetopause should enable boundary motion to be directly remote sensed for the first time. Indirect remote sensing capabilities might be enabled through the field-aligned currents associated with disturbances to the magnetopause; by harnessing data from satellite mega-constellations in low-Earth orbit, and taking advantage of upgraded auroral imaging and ionospheric radar technology. Finally, increased numbers of closely-spaced ground magnetometers in both hemispheres may help discriminate between high-latitude processes in what has previously been a "zone of confusion." Bringing together these multiple modes of observations for studying magnetopause dynamics is crucial. These may also be aided by advanced data processing techniques, such as physics-based inversions and machine learning methods, along with comparisons to increasingly sophisticated geospace assimilative models and simulations.

KEYWORDS

magnetopause, surface waves, MHD waves, auroral ionosphere, field-aligned currents, ground, instruments, techniques

1 Introduction

Earth's magnetopause, depicted in Figure 1A, is the interface of the solar–terrestrial interaction, hence mediates the flow of mass, momentum, and energy between the solar wind and geospace. As this interaction is responsible for the myriad of phenomena that can severely impact vital infrastructure, collectively known as space weather, understanding physical processes at the magnetopause and their system-wide effects is of utmost importance. The magnetopause is observed to be in almost continual motion. Alongside magnetic reconnection (Dungey, 1961), the wave-like motion of the magnetopause constitutes one of the major energy transfer mechanisms in the solar–terrestrial interaction (Axford, 1964). These magnetopause motions affect auroral, ionospheric, outer radiation belt, and trapped magnetospheric plasmas — either directly or indirectly through associated ultra-low frequency (ULF) waves (e.g., Sibeck, 1990; Elkington, 2006).

The boundary location in steady state is dictated by a balance of pressures (thermal, magnetic, and dynamic) on both sides of the magnetopause. Imbalances which lead to magnetopause motion are typically thought of as being externally driven, e.g., by variations in the upstream flow pressure (Potemra et al., 1989; Sibeck et al., 1989; Francia et al., 1999; Viall et al., 2009), the velocity shear as the solar wind flows around the magnetosphere (Kelvin-Helmholtz Instability, KHI; Chandrasekhar, 1961; Faganello and Califano, 2017; Masson and Nykyri, 2018), or reconnection with the interplanetary magnetic field altering the dayside magnetic flux (Hill and Rassbach, 1975; Matlsev and Lyatsky, 1975). However, internal processes such as the drift-mirror instability may also generate pressure changes that drive boundary dynamics (Constantinescu et al., 2009; Nykyri et al., 2021). Several of these driving processes may occur simultaneously and even modify one another, making observations hard to disentangle (e.g., Ma et al., 2014; Di Matteo et al., 2022).

The wave-like motion of the magnetopause is well approximated by magnetohydrodynamic surface wave theory (see recent review of Archer et al., 2024). The interplay of inertial, damping, and restoring forces on the dayside magnetopause predicts a ~5–10 min response to direct driving (Smit, 1968; Freeman et al., 1995; Børve et al., 2011; Horaites et al., 2023) alongside resonant ~10–20 min standing surface waves from ionospheric reflection (Chen and Hasegawa, 1974; Plaschke and Glassmeier, 2011; Archer and Plaschke, 2015). In contrast, on the magnetopause flanks where KH-waves dominate, periodicities are shorter ~1–7 min (Lin et al., 2014; Kavosi and Raeder, 2015). Corresponding wavelengths along the boundary span a wide spatial range, ~1–15 R_E (Lin et al., 2014).

Since magnetopause dynamics couple across many regions of geospace, there are numerous means of directly and indirectly observing the processes occurring and their consequences. In this paper we outline current and future observational capabilities at Earth, grouped by different target regions of geospace. We highlight new/improved directions to the field for unveiling magnetopause dynamics across different modes of observation and how these may aid our understanding of the boundary's global importance to the geospace energy budget.

2 Solar wind – magnetosphere interface

2.1 Multi-point *in-situ* measurements

In-situ spacecraft provide measurements of the physical conditions present at their location, such as particle distributions/moments and (DC/AC) electric/magnetic fields. Single spacecraft cannot unambiguously separate variations in space and time. Four spacecraft are the minimum required to uniquely resolve 3D structure (Paschmann and Daly, 1998), methods for which have been applied to the Cluster, MMS, and THEMIS missions. These typically assume first-order derivatives and planar structures over spacecraft separation scales. For studying magnetopause dynamics, the times the boundary passed over each spacecraft allow estimation of its local thickness and motion (Paschmann et al., 2005; Plaschke et al., 2009). Furthermore, simultaneous observations around the moving boundary allow comparison of spatial patterns against theory (e.g., Hasegawa et al., 2004; Plaschke et al., 2013; Archer et al., 2019; 2021).

Multi-spacecraft missions to date have typically focused on one scale at a time (e.g., fluid/ion for Cluster, ion/electron for MMS), achieved through precisely-controlled formations. In contrast, upcoming missions such as HelioSwarm (Klein et al., 2023) and the Plasma Observatory concept (Retinò et al., 2022) instead propose semi-autonomous swarms of 7+ spacecraft broadly separated across a variety of plasma scales. Swarms will allow unprecedented spatiotemporal reconstruction of magnetopause dynamics, e.g., KH roll-up vortices as in Figure 1C, while also probing important cross-scale physics.

While multi-spacecraft missions provide great detail of local structures and physical processes, geospace constitutes a "system of systems" with many different plasma populations that feedback on one another leading to more complex emergent/collective dynamical behaviour (Kepko, 2018; Kepko et al., 2023). This highlights the need for simultaneous observations across multiple spatial scales to understand how collective interactions produce "mesoscale" phenomena (~1–3 R_E in the magnetosphere) that mediate the global solar–terrestrial interaction.

Conjunctions between existing missions have revealed some of these feedbacks and mesoscale structuring relevant to magnetopause dynamics. For example, foreshock and magnetosheath transients emerge from interactions of large-scale solar wind structures with the quasi-parallel bow shock and reflected suprathermal foreshock ion populations, leading to many localised disturbances of the boundary and impacts throughout geospace (e.g., Archer et al., 2012; 2013; Nykyri et al., 2019; Wang et al., 2020a; Escoubet et al., 2020). Currently an extraordinary number of spacecraft orbit Earth, meaning many opportunities for multi-mission conjunctions exist. Indeed, Figure 1B highlights how March 2024 regularly offered simultaneous observations upstream of the bow shock, near the magnetopause at different local times, and at different *L*-shells within the magnetosphere.

Unfortunately, sparse conjunctions do not provide sufficient measurements to resolve all key processes across the "system of systems". Furthermore, care must be taken when comparing/combining measurements across different missions/instruments. Mission concepts for ~40 distributed

10.3389/fspas.2024.1430099

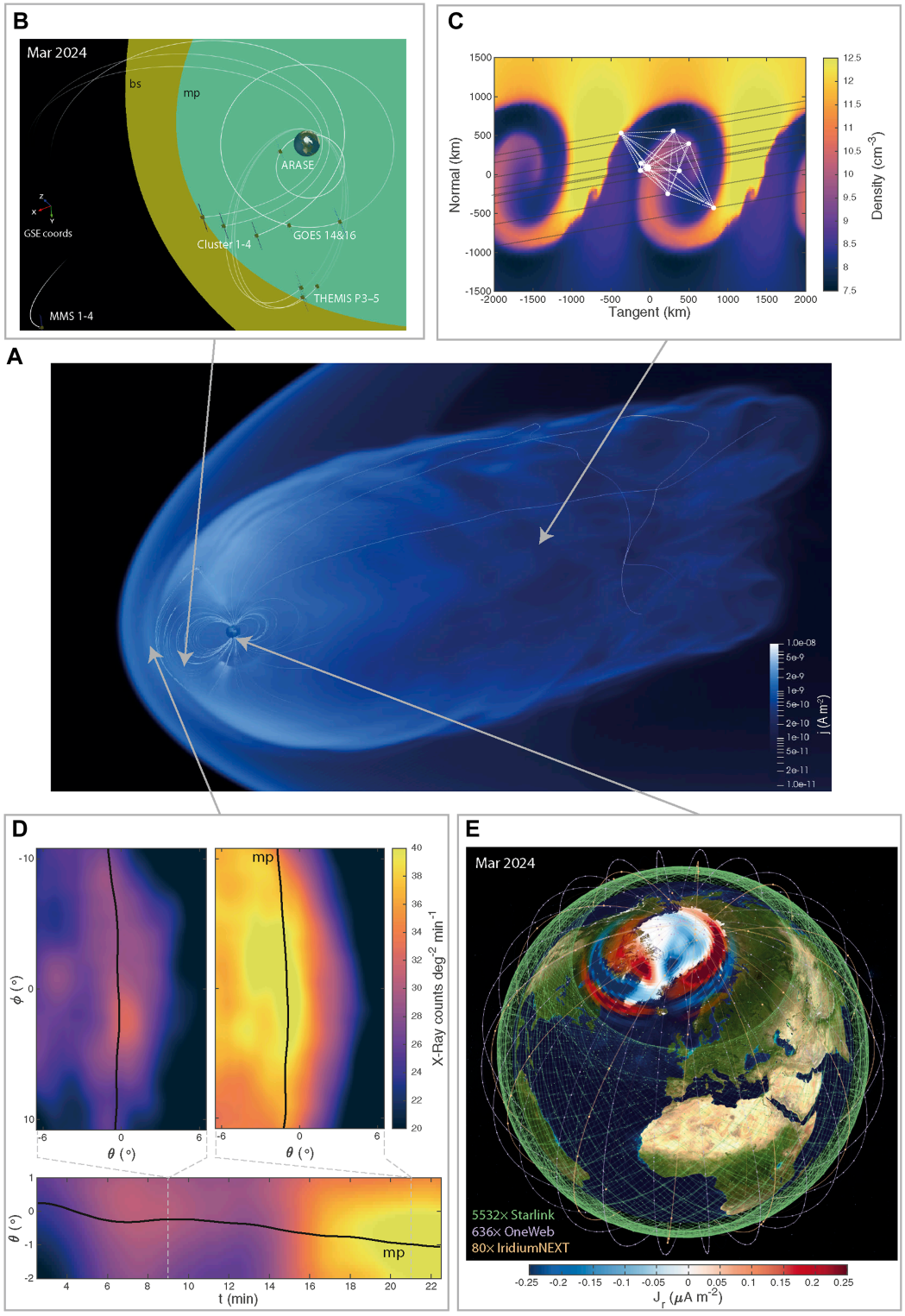

FIGURE 1
Current and future observational capabilities for studying magnetopause dynamics from space. **(A)** Visualisation of the magnetosphere from a Gorgon global MHD simulation (e.g., Mejnertsen et al., 2017). Displayed are volumetric current densities throughout the simulation, along with magnetic field lines in the meridional plane. **(B)** Example of an orbital conjunction from current *in-situ* missions ideal for investigating magnetopause dynamics. **(C)** Diagram of HelioSwarm skimming Kelvin-Helmholtz vortices from a local MHD simulation with 100 km velocity shear layer and no magnetic shear (Ma et al., 2017). **(D)** Simulated SMILE soft X-ray images (top panels) and time evolution along the Sun-Earth line (bottom panels) using data from Samsonov et al. (2024). The counts have been processed using multidimensional kernel density estimation, applying Epanechnikov kernels of optimal bandwidth from Silverman's rule (Silverman, 1986). A proxy for the magnetopause (black) is identified as the median of the marginal distributions. **(E)** Orbits of the Starlink, OneWeb, and Iridium NEXT constellations in low Earth orbit along with field-aligned currents associated with magnetopause surface waves from an SWMF global MHD simulation of the magnetospheric response to a solar wind density pulse (Archer et al., 2023).

identical spacecraft separated over "mesoscales" have been suggested to address this (Kepko, 2018; Kepko et al., 2023). These would have clear applications in building a global picture of magnetopause dynamics, revolutionising our understanding of the boundary's role in controlling mass, momentum, and energy transfer.

2.2 Soft X-rays

Large-scale imaging of the dynamic solar–terrestrial interaction from space is an emerging direction that clearly complements *in-situ* spacecraft and ground-based measurements. Several upcoming missions aim to image the dayside magnetosphere in soft X-rays from solar wind charge exchange, including the joint ESA-CAS SMILE mission (Branduardi-Raymont and Wang, 2022; Wang and Branduardi-Raymont, 2022), and smallsats Geo-X (Ezoe et al., 2020) and LEXI (Walsh et al., 2024). A heavy solar wind ion in the magnetosheath/cusps gains an electron in a high-energy state from a neutral exospheric atom, subsequently relaxing by emitting an X-ray photon (Cravens et al., 2001; Robertson and Cravens, 2003). Soft X-ray emissivities are predicted to peak at the tangent to the magnetopause (Sibeck et al., 2018), potentially enabling boundary dynamics to be tracked in both space and time.

Methods to determine the location of the magnetopause from X-ray images are not trivial, typically assuming some global shape (Samsonov et al., 2022; Wang and Sun, 2022). Furthermore, under typical to moderate solar wind driving, rather low photon counts are expected. Spatiotemporal binning can help increase signal-to-noise, though bins of scales comparable to typical dayside magnetopause motion ($1° \times 1° \times 5$ min) still result in very noisy images (e.g., Samsonov et al., 2022; 2024). While this may be mitigated by longer integration times and/or larger pixels, it would render boundary dynamics indeterminable.

More advanced techniques are likely required to improve scientific return. For example, data-driven density estimation techniques little used in our field may help (e.g., Archer et al., 2015; 2017). Instead of sharp fixed pixels, density estimation sums over smooth functions centred on each observation. This has convergence and continuity benefits over binning, and methods for data-driven scaling of bandwidths already exist (Silverman, 1986). Figure 1D shows our application to simulated data from Samsonov et al. (2024), demonstrating clear improvements.

3 Magnetosphere–ionosphere interface

Information about disturbances to the magnetopause are communicated to the auroral ionosphere along magnetic field lines by field-aligned currents (FACs), carried by precipitating magnetospheric electrons (ions) and/or upwelling ionospheric ions (electrons) for upward (downward) currents (Elphic, 1988; Sibeck, 1990). Recent high-resolution global MHD simulations, shown in Figure 1E (Archer et al., 2023), suggest magnetopause surface waves' FACs have large latitudinal extents (~10°) via non-resonant coupling between the compressional and Alfvén modes, peaking at the inner edge of the magnetopause transition (typically a few degrees equatorward of the Open–Closed Boundary, OCB; Kozyreva et al., 2019). These FACs open the possibility of remote sensing magnetopause motion at the magnetosphere–ionosphere interface. Current LEO spacecraft (e.g., Swarm, Friis-Christensen et al., 2008; POES; Evans and Greer, 2000; DMSP; Kilcommons et al., 2017; Redmon et al., 2017; and CASSIOPE; Yau and James, 2015) enable observations of magnetic field, electric field, precipitating particle, and/or drift velocity perturbations; all of which may be associated with magnetopause dynamics (e.g., Horvath and Lovell, 2021). However, due to orbital mechanics, single satellites in LEO provide a predominantly spatial cut and cannot capture the ~1–20 min periodicities at a fixed point in space associated with magnetopause motion. GDC's 6-spacecraft will enable temporal evolution of important magnetosphere–ionosphere–thermosphere coupling processes to be captured (Akbari et al., 2024). In early mission phases when orbital planes at high-latitudes are closest in longitude — best for studying magnetopause-related dynamics — resolvable timescales will be limited by the spacing/time between satellites to ~2–4 min. Mega-constellations with many satellites in the same orbital plane are required to capture the full range of magnetopause periodicities at the magnetosphere–ionosphere interface.

In recent years, commercial mega-constellations with 10's–1000s of satellites have been launched into LEO. Figure 1E shows orbits of the three largest to date: Iridium, OneWeb, and Starlink. The AMPERE project has successfully demonstrated engineering magnetometers aboard the polar-orbiting Iridium constellation (orange) can provide FAC observations across the polar cap through spherical fits to measured perturbations (Anderson et al., 2000; Waters et al., 2019). This has provided great insight into the variability of Region-1 and -2 FACs (Milan et al., 2017), though the 30° spacecraft separation within each of the 6 orbital planes means only periodicities >16 min are resolvable. Larger mega-constellations might be leveraged in a similar way, enabling FACs from magnetopause dynamics to be captured. OneWeb (purple) also has polar orbits, but twice as many orbital planes as Iridium and only ~7° separation within these. Thus OneWeb might provide ~2 min resolution polar maps with double the azimuthal fidelity. Starlink (green) occupy mostly ~50° inclined orbits, but a minority of orbits do cross the polar cap. The sheer number of Starlink satellites means it could still yield improved coverage/resolution to Iridium. Of course these possibilities would involve significant technical challenges and further developed processing methods, but could significantly advance our global monitoring of the dynamic solar–terrestrial interaction from space.

4 Ionosphere

4.1 Auroral imaging

Magnetopause disturbances can, through the precipitating magnetospheric particles carrying their FACs, lead to production/modulation of auroral emission in the ionosphere (e.g., Craven et al., 1986; Sibeck et al., 1999; Kozyreva et al., 2019). Aurorae are monitored from both ground and space, providing yet further means of remote sensing magnetopause dynamics.

This is a historic era for ground-based auroral science, with unprecedented all-sky imager (ASI) coverage operating coast-to-coast across the high latitude North American landscape, as shown

in Figure 2A (orange/yellow circles). The THEMIS-ASI network of 21 imagers (Donovan et al., 2006; 2008; Mende et al., 2008) has provided comprehensive panchromatic "white light" imaging since 2008, capturing qualitative images of auroral morphology from local to continent-wide scales (quantitative data can be derived by combining with meridian scanning photometers; Gabrielse et al., 2021). Since particle species cannot be differentiated in panchromatic data, aurorae are assumed caused by precipitating electrons. At 9 THEMIS-ASI sites are the REGO red-line imagers, which observe a key oxygen auroral emission (Liang et al., 2016). TREx, another continent-wide network across 6 locations (Gillies et al., 2019), instead features co-located monochromatic ASIs at major auroral emissions (blue-line, near-infrared, and RGB "true colour"). This enables electron flux and mean precipitation energy to be derived, yielding vital information on particle sources and their connection to the magnetosphere (Liang et al., 2022; 2024; Gillies et al., 2023). The THEMIS-ASIs are being replaced with RGB imagers to complement the SMILE mission, with the 19 new SMILE-ASIs completing by summer 2025 (Carter et al., 2024). Of course, ground-based auroral imagery is only possible during clear night skies, which for dayside magnetopause signatures limits studies to winter seasons.

In addition to ground-based imagers, space-based ones such as on IMAGE (Mende et al., 2000b; a,c), Polar (Torr et al., 1995), DMSP (Paxton et al., 2002), the upcoming SMILE (Branduardi-Raymont and Wang, 2022) and proposed MAAX (Halford et al., 2024) have the benefit of observing large areas and at wavelengths (e.g., UV-band) not observable from the ground. Furthermore, UV auroral observations are possible at all times, independent of light pollution. However, space-based auroral images are less detailed, due to trade-offs between spatial coverage and integration times, as well as orbital configuration. While DMSP auroral images build up over ~25 min polar crossings, meaning spatiotemporal ambiguity affects potential magnetopause signatures, both Polar and IMAGE were spinning allowing ~1–2 min cadence images, suitable for resolving auroral impacts of long-period magnetopause waves (e.g., Liou et al., 2008). SMILE's UVI will cover the entire auroral oval for the first time since 2005, allowing global auroral dynamics to be captured at 1 min and ~50–150 km resolution, augmented by more detailed imagery from the ground.

Figure 2B shows simulated FACs associated with magnetopause surface waves which may lead to auroral signatures (Archer et al., 2023). While auroral bright spots have been linked to the magnetopause (Lundin and Evans, 1985; Kozyreva et al., 2019) and recently plasmapause (He et al., 2020; Horvath and Lovell, 2021), it is not clear if surface waves' FACs are sufficient to generate emission or simply modulate existing aurorae. Insight might be gained through comparison with field line resonances, whose similar periodic FACs do produce aurorae (Samson et al., 1996; Milan et al., 2001; Gillies et al., 2018).

4.2 Radar

Closure of magnetopause disturbances' FACs through ionospheric Pedersen currents are associated with electric field oscillations and $\mathbf{E}\times\mathbf{B}$ plasma drifts, resulting in so-called Travelling Convection Vortices (TCVs, Friis-Christensen et al., 1988; Bristow et al., 1995) which may be detected by radar observations (e.g., Walsh et al., 2015; Shi et al., 2020).

SuperDARN (e.g., Ruohoniemi et al., 1989; Ruohoniemi and Greenwald, 1996; Chisham et al., 2007; Nishitani et al., 2019, etc.) consists of ground-based high-frequency coherent scatter radars which measure line-of-sight Doppler shifts of ionospheric irregularities. The network has expanded over the past 2 decades/solar cycles across high- (blue/red fans in Figure 2A) and mid-latitudes, enabling coverage for typical but also disturbed geomagnetic conditions (Nishitani et al., 2019; Walach and Grocott, 2019; Walach et al., 2021). Historically, ULF waves have been studied at individual radars, where comparing measurements across multiple beams (see Figure 2C for simulated single-beam observations) can track 2-D wave propagation providing insights into drivers (Fenrich et al., 1995; James et al., 2013). Because a full scan of the SuperDARN field-of-view took ~1–2 min though, signatures due to faster magnetopause dynamics (e.g., KH-waves) could not be fully captured over large-scales. However, exciting upgrades to digital radar systems (e.g., McWilliams et al., 2023) are enabling imaging at 3.5 s resolution. As these improvements roll out, the overlapping fields-of-view might allow unprecedented large-scale observations of TCVs due magnetopause dynamics through high-order spherical fits to velocity measurements (Ruohoniemi et al., 1989).

In addition to coherent scatter radars, Incoherent Scatter Radar (ISR, cyan stars in Figure 2A), e.g., EISCAT (Rietveld et al., 2019; Stamm et al., 2021), PFISR (Nicolla and Heinselman, 2007), and RISR, (Gillies et al., 2016), is another valuable tool for remote sensing magnetopause dynamics from the ionosphere. Buchert et al. (1999) and Wang et al. (2020b) used ISR measurements showing ULF waves with periods from 1–10 min significantly modulate the ionospheric electron density at a range of altitudes, ultimately affecting ionospheric conductance. While ISR's spatial coverage is limited for resolving the spatial scales and propagation of magnetopause dynamics, its ability to offer insights into altitude profiles of multiple ionospheric parameters becomes invaluable. These are aspects poorly explored both in magnetopause dynamical theory/simulations and observations at present.

4.3 Global navigation satellite systems (GNSS)

Ionospheric total electron content (TEC), the columnar number density, is most widely obtained using remote-sensing techniques between GNSS satellites and ground-receivers (magenta dots in Figure 2A). Observed TEC fluctuations with periods 10–1000 s have been linked to ULF waves in the polar cap (e.g., Watson et al., 2016), auroral zone (e.g., Pilipenko et al., 2014), and mid-/low-latitude regions (e.g., Yizengaw et al., 2018). These have amplitudes as large as 7 TECU (Watson et al., 2015). Pilipenko et al. (2014) explored several possible mechanisms of higher latitude ULF wave driven TEC fluctuations, two of which may be related to magnetopause surface waves and have been invoked in other studies. These are wave-modulated precipitation of energetic electrons affecting ionospheric conductivities (Buchert et al., 1999; Wang et al., 2020b), and periodic vertical plasma flows due

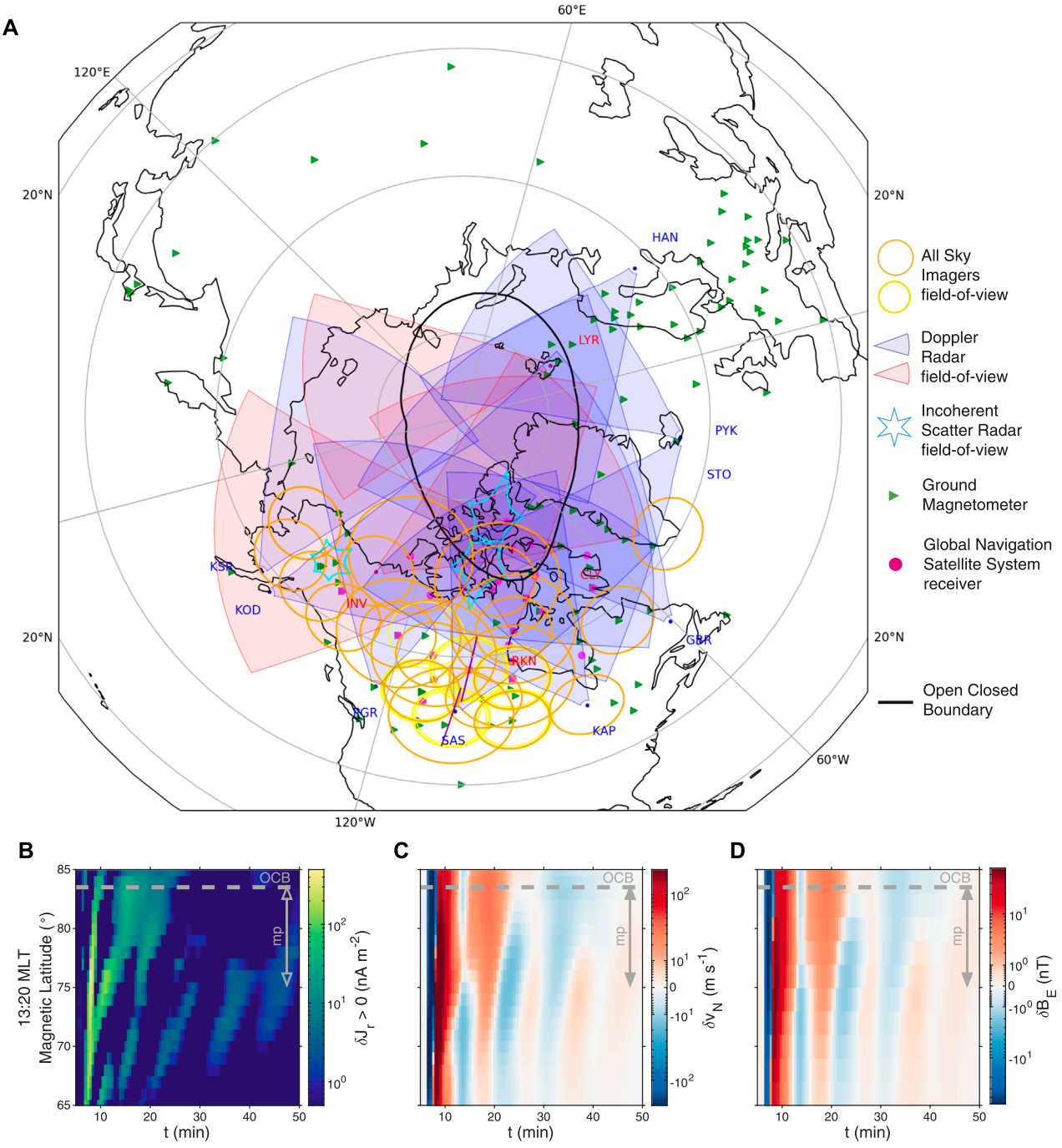

FIGURE 2
Current observational capabilities for remote sensing magnetopause dynamics and their impacts from the ground. **(A)** Orthographic map showing ground-based instruments in the high-latitude northern hemisphere in geographic coordinates (20° latitudinal spacing). These include SuperDARN radars (red/blue fans), SuperMAG ground magnetometers (green triangles), All Sky Imagers (orange/yellow circles), Incoherent Scatter Radar (cyan stars), spectrograph fields (purple lines), and Chain GNSS receivers (magenta dots). The Open–Closed Boundary (OCB) from the Tsyganenko (1995) model under median conditions is shown as the thick black line. Panels **(B–D)** Potential dayside ground-based signatures of magnetopause surface waves from the same global MHD simulation as in Figure 1E. Displayed are magnetic latitude–time plots (keograms) of perturbations in upwards field-aligned currents **(B)**, North–South ionospheric velocity **(C)**, and East–West ground magnetic field **(D)** near the noon sector. The OCB (dashed grey lines) and projected extent of the magnetopause (double-headed arrows) from the simulation are also displayed (note global simulation numerics lead to more smeared out boundary layers than in reality).

to waves' FACs (Belakhovsky et al., 2016; Kozyreva et al., 2020). TEC observations are complicated by satellite orbits and line-of-sight, with standard conversions from "slant" to "vertical" TEC (e.g., Kozyreva et al., 2020) assuming homogeneity over ~10° — invalid for even large-scale surface waves (Archer et al., 2023). Further modelling to better understand the physical

processes behind TEC fluctuations and any observational biases are needed for GNSS to become a valuable remote-sensing tool for magnetopause dynamics.

5 Ground magnetic field

The magnetic field at Earth's surface includes contributions from magnetosphere–ionosphere currents. Global networks of ground-based magnetometers of varying spatial separations (> 200 km, green triangles in Figure 2A) have been some of the earliest and most widely used tools for understanding how magnetopause disturbances lead to FACs/waves (Friis-Christensen et al., 1988; Sibeck, 1990; Araki, 1994; Motoba et al., 2007), ultimately impacting the global magnetosphere–ionosphere–thermosphere system (e.g., Shi et al., 2022). While unable to detect phenomena < 100 km (Hughes and Southwood, 1976), they have a few important advantages over other instruments. They can operate continuously without concern for sunlight, cloud cover, and ionospheric backscatter. Closely spaced magnetometers can also resolve important mesoscales from the ground (Engebretson and Zesta, 2017). Furthermore, ground magnetometers do not move in the geocentric frame, thus the interpretation of their data is less complicated than satellites (e.g., Anderson et al., 1989).

Studies of high-latitude ULF waves have been described as a "zone of confusion" with structuring whose relation out to the magnetosphere is ambiguous (Pilipenko et al., 2015; 2018; see also Figure 2D). Unambiguously linking wave power enhancements with magnetopause surface waves (e.g., Glassmeier, 1992), or other wave activity (e.g., Araki and Nagano, 1988; Lyatsky and Sibeck, 1997), may require closely spaced networks of magnetometers to identify the polarization changes and wave power variations predicted by simulations (Archer et al., 2023). 2D networks in both hemispheres spanning the cusp and auroral zones would further help discriminate wave modes; e.g., enabling natural experiments for isolating surface wave signatures from telluric currents (Weygand et al., 2023), variations in ionospheric conductance (e.g., Hartinger et al., 2017), and asymmetries in upstream driving conditions (e.g., Oliveira et al., 2020; Shi et al., 2020; Di Matteo and Sivadas, 2022; Villante et al., 2022).

Finally, magnetotelluric survey networks (e.g., USArray's EarthScope sites; Schultz, 2010) consist of small arrays taking simultaneous geoelectric and geomagnetic field measurements temporarily (typically ~3 weeks, but variable), subsequently moving locations. They have a few unique capabilities relevant for surface wave diagnostics (Hartinger et al., 2020; Shi et al., 2022). They are typically deployed in more spatially dense networks than typical magnetometer networks (< 70 km) thus capture finer-scale features. They provide information about ground conductivity, which can be used to discriminate magnetosphere–ionosphere currents from telluric currents. They also yield additional geoelectric field measurements, enabling the waves' hazard to power systems to be considered. However, their spatial coverage at any given time is much more limited and site locations may not always be optimal for studying the magnetopause's effects on the ground.

6 Discussion

This is an exciting time for studying magnetopause dynamics, with many new/emerging observational capabilities in both *in-situ* and remote sensing measurements. Each of these enables us to probe the physical processes occurring at the boundary and their impacts upon geospace. While each observational method has its own unique benefits and drawbacks, bringing them together simultaneously will start to provide a holistic view of the magnetopause's controlling role in mediating the solar–terrestrial interaction — from local physics, through to emergent mesoscale features, and ultimately the collective global response/impact. It is crucial this unprecedented observational coverage be maintained through sustained funding for extended mission/instrumentation operations.

Along with this unprecedented diversity and coverage of measurements, data processing methods will become more important than ever. Inversion techniques applied to multi-point measurements offer unique opportunities to resolve the temporal evolution and spatial structure of different wave modes, which may otherwise be convolved in original datasets complicating their physical interpretation (Archer et al., 2023). For example, distributed 2D networks of ground-based magnetometers have long been used to obtain magnetospheric field-aligned, ionospheric Pedersen and Hall, and now even telluric currents via the Spherical Elementary Current System technique (e.g., Shi et al., 2022; Weygand et al., 2023). Similar methods are now also being applied to SuperDARN observations (e.g., Fenrich et al., 2019). These approaches may further be boosted through machine learning capabilities (Camporeale, 2019; Nguyen et al., 2022; Grimmich et al., 2023), allowing more sophisticated data analysis across "big data" for the identification of signals related to magnetopause surface waves and dynamics (e.g., Cicone et al., 2016; Murphy et al., 2020; Di Matteo et al., 2021), especially in nonlinear and nonstationary contexts (Piersanti et al., 2018; Stallone et al., 2020). Finally, data mining and assimilation (Tsyganenko and Sitnov, 2007; Merkin et al., 2016; Alzate et al., 2023) into maturing "system of systems" models (e.g., Zhang et al., 2019; Sorathia et al., 2020; 2023; Gombosi et al., 2021) can aid the interpretation of this unprecedented, but still scattered, data collection enabling the global context to be inferred.

The techniques and physical insights gained from studying Earth's magnetopause might also translate to different space plasma environments where fewer observational methods are possible, such as the other planetary magnetopauses (e.g., Masters et al., 2009; Boardsen et al., 2010; Montgomery et al., 2023) or solar coronal structures like loops (Nakariakov et al., 2016). Here similar dynamical processes are thought to occur but over vastly different scales, morphologies, and/or plasma conditions.

Data availability statement

The original contributions presented in the study are included in the article/supplementary material, further inquiries can be directed to the corresponding author.

Author contributions

MA: Conceptualization, Funding acquisition, Visualization, Writing–original draft, Writing–review and editing. XS: Conceptualization, Visualization, Writing–original draft, Writing–review and editing. M-TW: Conceptualization, Writing–original draft, Writing–review and editing. MH: Conceptualization, Writing–original draft, Writing–review and editing. DG: Conceptualization, Writing–original draft, Writing–review and editing. SD: Conceptualization, Writing–original draft, Writing–review and editing. FS: Conceptualization, Writing–review and editing. KN: Funding acquisition, Writing–review and editing.

Funding

The author(s) declare that financial support was received for the research, authorship, and/or publication of this article. This work was supported by the International Space Science Institute (ISSI) in Bern, through ISSI International Team project #546 "Magnetohydrodynamic Surface Waves at Earth's Magnetosphere (and Beyond)." MA was supported by UKRI (STFC/EPSRC) Stephen Hawking Fellowship EP/T01735X/1 and UKRI Future Leaders Fellowship MR/X034704/1. XS was supported by National Aeronautics and Space Administration (NASA) awards 80NSSC21K1677 and 80NSSC21K1683, National Science Foundation (NSF) awards AGS-1935110, AGS-2025570, and AGS-2307205. M-TW was supported by UKRI (STFC) Ernest Rutherford Fellowship ST/X003663/1. MH was supported by NASA awards 80NSSC21K1683 and 80NSSC23K0903, and NSF awards AGS-2307204 and AGS-2027210. SD was supported by NASA award 80NSSC21K0459. FS was supported by NASA award 80NSSC21K0448.

Acknowledgments

We acknowledge the 3DView online tool (Génot et al., 2018) used to create Figure 1B. We acknowledge the pyDARN package (Shi et al., 2022) used to create Figure 2A. For the purpose of open access, the author(s) has applied a Creative Commons attribution (CC BY) licence to any Author Accepted Manuscript version arising.

Conflict of interest

The authors declare the absence of any commercial or financial relationships that could be construed as a potential conflict of interest.

The author(s) declared that they were an editorial board member of Frontiers, at the time of submission. This had no impact on the peer review process and the final decision.

Publisher's note

References

Akbari, H., Rowland, D., Coleman, A., Buynovskiy, A., and Thayer, J. (2024). Gradient calculation techniques for multi-point ionosphere/thermosphere measurements from GDC. *Front. Astron. Space Sci.* 11, 1231840. doi:10.3389/fspas.2024.1231840

Alzate, N., Di Matteo, S., Morgan, H., Seaton, D. B., Miralles, M. P., Balmaceda, L., et al. (2023). Data mining for science of the sun-earth connection as a single system. *Front. Astronomy Space Sci.* 10, 1151785. doi:10.3389/fspas.2023.1151785

Anderson, B. J., Engebretson, M. J., and Zanetti, L. J. (1989). Distortion effects in spacecraft observations of MHD toroidal standing waves: theory and observations. *J. Geophys. Res.* 94, 13425–13445. doi:10.1029/JA094iA10p13425

Anderson, B. J., Takahashi, K., and Toth, B. A. (2000). Sensing global Birkeland currents with iridium® engineering magnetometer data. *Geophys. Res. Lett.* 27, 4045–4048. doi:10.1029/2000GL000094

Araki, T. (1994). A Physical model of the geomagnetic sudden commencement. *Geophys. Monogr. Ser.* 81, 183–200. doi:10.1029/GM081p0183

Araki, T., and Nagano, H. (1988). Geomagnetic response to sudden expansions of the magnetosphere. *J. Geophys. Res. Space Phys.* 93, 3983–3988. doi:10.1029/JA093iA05p03983

Archer, M. O., Hartinger, M. D., Plaschke, F., Southwood, D. J., and Rastaetter, L. (2021). Magnetopause ripples going against the flow form azimuthally stationary surface waves. *Nat. Commun.* 12, 5697. doi:10.1038/s41467-021-25923-7

Archer, M. O., Hartinger, M. D., Rastaetter, L., Southwood, D. J., Heyns, M., Eggington, J. W. B., et al. (2023). Auroral, ionospheric and ground magnetic signatures of magnetopause surface modes. *J. Geophys. Res. Space Phys.* 128, e2022JA031081. doi:10.1029/2022JA031081

Archer, M. O., Hartinger, M. D., Walsh, B. M., and Angelopoulos, V. (2017). Magnetospheric and solar wind dependences of coupled fast-mode resonances outside the plasmasphere. *J. Geophys. Res. Space Phys.* 122, 212–226. doi:10.1002/2016JA023428

Archer, M. O., Hartinger, M. D., Walsh, B. M., Plaschke, F., and Angelopoulos, V. (2015). Frequency variability of standing alfvén waves excited by fast mode resonances in the outer magnetosphere. *Geophys. Res. Lett.* 42, 10150–10159. doi:10.1002/2015GL066683

Archer, M. O., Hietala, H., Hartinger, M. D., Plaschke, F., and Angelopoulos, V. (2019). Direct observations of a surface eigenmode of the dayside magnetopause. *Nat. Commun.* 10, 615. doi:10.1038/s41467-018-08134-5

Archer, M. O., Horbury, T. S., and Eastwood, J. P. (2012). Magnetosheath pressure pulses: generation downstream of the bow shock from solar wind discontinuities. *J. Geophys. Res. Spoace Phys.* 117, A05228. doi:10.1029/2011JA017468

Archer, M. O., Horbury, T. S., Eastwood, J. P., Weygand, J. M., and Yeoman, T. K. (2013). Magnetospheric response to magnetosheath pressure pulses: a low pass filter effect. *J. Geophys. Res. Space Phys.* 118, 5454–5466. doi:10.1002/jgra.50519

Archer, M. O., Pilipenko, V. A., Li, B., Sorathia, K., Nakariakov, V. M., Elsden, T., et al. (2024). Magnetopause MHD surface wave theory: progress & challenges. *Front. Astron. Space Sci.* 11. In press. doi:10.3389/fspas.2024.1407172

Archer, M. O., and Plaschke, F. (2015). What frequencies of standing surface waves can the subsolar magnetopause support? *J. Geophys Res.* 120, 3632–3646. doi:10.1002/2014JA020545

Axford, W. I. (1964). Viscous interaction between the solar wind and the earth's magnetosphere. *Planet. Space Sci* 12, 45–53. doi:10.1016/0032-0633(64)90067-4

Belakhovsky, V., Pilipenko, V., Murr, D., Fedorov, E., and Kozlovsky, A. (2016). Modulation of the ionosphere by pc5 waves observed simultaneously by gps/tec and eiscat. *Earth, Planets Space* 68, 102–113. doi:10.1186/s40623-016-0480-7

Boardsen, S. A., Sundberg, T., Slavin, J. A., Anderson, B. J., orth, H., Solomon, S. C., et al. (2010). Observations of Kelvin-Helmholtz waves along the dusk-side boundary of Mercury's magnetosphere during MESSENGER's third flyby. *Gephys. Res. Lett.* 37, L12101. doi:10.1029/2010GL043606

Børve, S., Sato, H., Pécseli, H. L., and Trulsen, J. K. (2011). Minute-scale period oscillations of the magnetosphere. *Ann. Geophys.* 29, 663–671. doi:10.5194/angeo-29-663-2011

Branduardi-Raymont, G., and Wang, C. (2022). *The SMILE mission*. Singapore: Springer Nature Singapore, 1–22. doi:10.1007/978-981-16-4544-0_39-1

Bristow, W. A., Sibeck, D. G., Jacquey, C., Greenwald, R. A., Sofko, G. J., Mukai, T., et al. (1995). Observations of convection vortices in the afternoon sector using the SuperDARN HF radars. *J. Geophys. Res. Space Phys.* 100, 19743–19756. doi:10.1029/95JA01301

Buchert, S. C., Fujii, R., and Glassmeier, K.-H. (1999). Ionospheric conductivity modulation in ULF pulsations. *J. Geophys. Res. Space Phys.* 104, 10119–10133. doi:10.1029/1998JA900180

Camporeale, E. (2019). The challenge of machine learning in space weather: nowcasting and forecasting. *Space weather.* 17, 1166–1207. doi:10.1029/2018SW002061

Carter, J. A., Dunlop, M., Forsyth, C., Oksavik, K., Donovon, E., Kavanagh, A., et al. (2024). Ground-based and additional science support for SMILE. *Earth Planet. Phys.* 8, 275–298. doi:10.26464/epp2023055

Chandrasekhar, S. (1961). *Hydrodynamic and hydromagnetic stability*. Oxford, UK: Oxford University Press.

Chen, L., and Hasegawa, A. (1974). A theory of long-period magnetic pulsations: 2. impulse excitation of surface eigenmode. *J. Geophys. Res.* 79, 1033–1037. doi:10.1029/JA079i007p01033

Chisham, G., Lester, M., Milan, S. E., Freeman, M. P., Bristow, W. a., Grocott, a., et al. (2007). A decade of the super dual auroral radar network (SuperDARN): scientific achievements, new techniques and future directions. *Surv. Geophys.* 28, 33–109. doi:10.1007/s10712-007-9017-8

Cicone, A., Liu, L., and Zhou, H. (2016). Adaptive local iterative filtering for signal decomposition and instantaneous frequency analysis. *Appl. Comput. Harmon. Analysis* 41, 384–411. doi:10.1016/j.acha.2016.03.001

Constantinescu, O. D., Glassmeier, K.-H., Plaschke, F., Auster, U., Angelopoulos, V., Baumjohann, W., et al. (2009). THEMIS observations of duskside compressional Pc5 waves. *J. Geophys. Res. Space Phys.* 114, A00C25. doi:10.1029/2008JA013519

Craven, J. D., Frank, L. A., Russell, C. T., Smith, E. J., and Lepping, R. P. (1986). *Solar Wind-Magnetosphere Coupling (Tokyo, Japan: terra Sci.), chap. Global auroral responses to magnetospheric compressions by shocks in the solar wind*, 367–380.

Cravens, T. E., Robertson, I. P., and Snowden, S. L. (2001). Temporal variations of geocoronal and heliospheric X-ray emission associated with the solar wind interaction with neutrals. *J. Geophys. Res. Space Phys.* 106, 24883–24892. doi:10.1029/2000JA000461

Di Matteo, S., and Sivadas, N. (2022). Solar-wind/magnetosphere coupling: understand uncertainties in upstream conditions. *Front. Astronomy Space Sci.* 9, 333. doi:10.3389/fspas.2022.1060072

Di Matteo, S., Viall, N. M., and Kepko, L. (2021). Power spectral density background estimate and signal detection via the multitaper method. *J. Geophys. Res. Space Phys.* 126, e28748. doi:10.1029/2020ja028748

Di Matteo, S., Villante, U., Viall, N., Kepko, L., and Wallace, S. (2022). On differentiating multiple types of ULF magnetospheric waves in response to solar wind periodic density structures. *J. Geophys. Res. Space Phys.* 127, e2021JA030144. doi:10.1029/2021ja030144

Donovan, E., Liu, W., Liang, J., Spanswick, E., Voronkov, I., Connors, M., et al. (2008). Simultaneous THEMIS *in situ* and auroral observations of a small substorm, *Geophys. Res. Lett.*, 35, L17S18. doi:10.1029/2008GL033794

Donovan, E., Mende, S., Jackel, B., Frey, H., Syrjäsuo, M., Voronkov, I., et al. (2006). The THEMIS all-sky imaging array—system design and initial results from the prototype imager. *J. Atmos. Solar-Terrestrial Phys.* 68, 1472–1487. doi:10.1016/j.jastp.2005.03.027

Dungey, J. W. (1961). Interplanetary magnetic field and the auroral zones. *Phys. Rev. Lett.* 6, 47–48. doi:10.1103/PhysRevLett.6.47

Engebretson, M., and Zesta, E. (Editors) (2017). *Ground magnetometer array planning: report of a workshop*. Minneapolis, USA: Augsburg College. http://space.augsburg.edu/GroundMagnetometerWorkshopReport.pdf

Elkington, S. R. (2006). "A review of ULF interactions with radiation belt electrons,". Editors K. Takahashi, P. J. Chi, R. E. Denton, and R. L. Lysak (John Wiley & Sons), 169.*Magnetospheric ULF waves: synthesis and new directions*

Elphic, R. C. (1988). Multipoint observations of the magnetopause: results from ISEE and AMPTE. *Adv. Space Res.* 8, 223–238. doi:10.1016/0273-1177(88)90135-4

Escoubet, C. P., Hwang, K.-J., Toledo-Redondo, S., Turc, L., Haaland, S. E., Aunai, N., et al. (2020). Cluster and MMS simultaneous observations of magnetosheath high speed jets and their impact on the magnetopause. *Front. Astron. Space Sci.* 6, 78. doi:10.3389/fspas.2019.00078

Evans, D. S., and Greer, M. S. (2000) "*Polar orbiting environmental satellite space environment monitor—2: instrument descriptions and archive data documentation*,". Boulder, CO, USA: NOAA.

Ezoe, Y., Funase, R., Nagata, H., Miyoshi, Y., Kasahara, S., Nakajima, H., et al. (2020). "GEO-X (GEOspace x-ray imager),". *Space telescopes and instrumentation 2020: ultraviolet to gamma ray*. Editors J.-W. A. den Herder, S. Nikzad, and K. Nakazawa (SPIE: International Society for Optics and Photonics), 11444. doi:10.1117/12.25607801144428

Faganello, M., and Califano, F. (2017). Magnetized Kelvin–Helmholtz instability: theory and simulations in the earth's magnetosphere context. *J. Plasma Phys.* 83, 535830601. doi:10.1017/S0022377817000770

Fenrich, F. R., Gillies, D. M., Donovan, E., and Knudsen, D. (2019). Flow velocity and field-aligned current associated with field line resonance: SuperDARN measurements. *J. Geophys. Res. Space Phys.* 124, 4889–4904. doi:10.1029/2019JA026529

Fenrich, F. R., Samson, J. C., Sofko, G., and Greenwald, R. A. (1995). ULF high- and low-m field line resonances observed with the super dual auroral radar network. *J. Geophys. Res. Space Phys.* 100, 21535–21547. doi:10.1029/95JA02024

Francia, P., Lepidi, S., Villante, U., Di Giuseppe, P., and Lazarus, A. J. (1999). Geomagnetic response at low latitude to continuous solar wind pressure variations during northward interplanetary magnetic field. *J. Geophys. Res. Space Phys.* 104, 19923–19930. doi:10.1029/1999JA900229

Freeman, M. P., Freeman, N. C., and Farrugia, C. J. (1995). A linear perturbation analysis of magnetopause motion in the Newton-Busemann limit. *Ann. Geophys.* 13, 907–918. doi:10.1007/s00585-995-0907-0

Friis-Christensen, E., Lühr, H., Knudsen, D., and Haagmans, R. (2008). Swarm – an earth observation mission investigating geospace. *Adv.Space Res.* 41, 210–216. doi:10.1016/j.asr.2006.10.008

Friis-Christensen, E., McHenry, M. A., Clauer, C. R., and Vennerstrøm, S. (1988). Ionospheric traveling convection vortices observed near the polar cleft: a triggered response to sudden changes in the solar wind. *Geophys. Res. Lett.* 15, 253–256. doi:10.1029/GL015i003p00253

Gabrielse, C., Nishimura, T., Chen, M., Hecht, J. H., Kaeppler, S. R., Gillies, D. M., et al. (2021). Estimating precipitating energy flux, average energy, and Hall auroral conductance from THEMIS all-sky-imagers with focus on mesoscales. *Front. Phys.* 9, 744298. doi:10.3389/fphy.2021.744298

Génot, V., Beigbeder, L., Popescu, D., Dufourg, N., Gangloff, M., Bouchemit, M., et al. (2018). Science data visualization in planetary and heliospheric contexts with 3DView. *Planet. Space Sci.* 150, 111–130. doi:10.1016/j.pss.2017.07.007

Gillies, D. M., Donovan, E., Hampton, D., Liang, J., Connors, M., Nishimura, Y., et al. (2019). First observations from the TREx spectrograph: the optical spectrum of STEVE and the picket fence phenomena. *Geophys. Res. Lett.* 46, 7207–7213. doi:10.1029/2019GL083272

Gillies, D. M., Knudsen, K., Rankin, R., Milan, S., and Donovan, E. (2018). A statistical survey of the 630.0-nm optical signature of periodic auroral arcs resulting from magnetospheric field line resonances. *Geophys. Res. Lett.* 45, 4648–4655. doi:10.1029/2018GL077491

Gillies, D. M., Liang, J., Gallardo-Lacourt, B., and Donovan, E. (2023). New insight into the transition from a SAR arc to STEVE. *Geophys. Res. Lett.* 50, e2022GL101205. doi:10.1029/2022GL101205

Gillies, R. G., van Eyken, A., Spanswick, E., Nicolls, M., Kelly, J., Greffen, M., et al. (2016). First observations from the RISR-C incoherent scatter radar. *Radio Sci.* 51, 1645–1659. doi:10.1002/2016RS006062

Glassmeier, K.-H. (1992). Traveling magnetospheric convection twin-vortices: observations and theory. *Ann. Geophys.* 10.

Gombosi, T. I., Chen, Y., Glocer, A., Huang, Z., Jia, X., Liemohn, M. W., et al. (2021). What sustained multi-disciplinary research can achieve: the space weather modeling framework. *J. Space Weather Space Clim.* 11, 42. doi:10.1051/swsc/2021020

Grimmich, N., Plaschke, F., Archer, M. O., Heyner, D., Mieth, J. Z. D., Nakamura, R., et al. (2023). Study of extreme magnetopause distortions under varying solar wind conditions. *J. Geophys. Res. Space Phys.* 128, e2023JA031603. doi:10.1029/2023JA031603

Halford, A., Liemohn, M., Ridley, A., Welling, D., Immel, T., Connor, H., et al. (2024) "Magnetospheric Auroral Asymmetry eXplorer: observing the auroral to uncover how energy flows in space-A Phase A SMEX Mission concept,". Abstract No. EGU24-2058. Göttingen, Germany: Copernicus Meetings.

Hartinger, M. D., Shi, X., Lucas, G. M., Murphy, B. S., Kelbert, A., Baker, J. B. H., et al. (2020). Simultaneous observations of geoelectric and geomagnetic fields produced by magnetospheric ULF waves. *Geophys. Res. Lett.* 47, e2020GL089441. doi:10.1029/2020GL089441

Hartinger, M. D., Xu, Z., Clauer, C. R., Yu, Y., Weimer, D. R., Kim, H., et al. (2017). Associating ground magnetometer observations with current or voltage generators. *J. Geophys. Res. Space Phys.* 122, 7130–7141. doi:10.1002/2017JA024140

Hasegawa, H., Fujimoto, M., Phan, T.-D., Rème, H., Balogh, A., Dunlop, M. W., et al. (2004). Transport of solar wind into Earth's magnetosphere through rolled-up Kelvin–Helmholtz vortices. *Nature* 430, 755–758. doi:10.1038/nature02799

He, F., Guo, R.-L., Dunn, W. R., Yao, Z.-H., Zhang, H.-S., Hao, Y.-X., et al. (2020). Plasmapause surface wave oscillates the magnetosphere and diffuse aurora. *Nat. Commun.* 11, 1668. doi:10.1038/s41467-020-15506-3

Hill, T. W., and Rassbach, M. E. (1975). Interplanetary magnetic field direction and the configuration of the day side magnetosphere. *J. Geophys. Res.* 80, 1–6. doi:10.1029/JA080i001p00001

Horaites, K., Rintamäki, E., Zaitsev, I., Turc, L., Grandin, M., Cozzani, G., et al. (2023). Magnetospheric response to a pressure pulse in a three-dimensional hybrid-vlasov simulation. *J. Geophys. Res. Space Phys.* 128, e2023JA031374. doi:10.1029/2023JA031374

Horvath, I., and Lovell, B. C. (2021). Subauroral flow channel structures and auroral undulations triggered by kelvin-helmholtz waves. *J. Geophys. Res. Space Phys.* 126, e2021JA029144. doi:10.1029/2021JA029144

Hughes, W. J., and Southwood, D. J. (1976). The screening of micropulsation signals by the atmosphere and ionosphere. *J. Geophys. Res.* 81, 3234–3240. doi:10.1029/JA081i019p03234

James, M. K., Yeoman, T. K., Mager, P. N., and Klimushkin, D. Y. (2013). The spatio-temporal characteristics of ULF waves driven by substorm injected particles. *J. Geophys. Res. Space Phys.* 118, 1737–1749. doi:10.1002/jgra.50131

Kavosi, S., and Raeder, J. (2015). Ubiquity of kelvin–helmholtz waves at earth's magnetopause. *Nat. Commun.* 6, 7019. doi:10.1038/ncomms8019

Kepko, L. (2018). "Magnetospheric constellation: leveraging space 2.0 for big science," in *Igarss 2018 - 2018 IEEE international geoscience and remote sensing symposium*, 285–288. doi:10.1109/IGARSS.2018.8519475

Kepko, L., Gabrielse, C., Gkioulidou, M., Nykyri, K., Sibeck, D., Turner, D., et al. (2023). Magnetospheric constellation (MagCon). *Bull. AAS* 55. doi:10.3847/25c2cfeb.0e470159Available at: https://baas.aas.org/pub/2023n3i200.

Kilcommons, L. M., Redmon, R. J., and Knipp, D. J. (2017). A new DMSP magnetometer and auroral boundary data set and estimates of field-aligned currents in dynamic auroral boundary coordinates. *J. Geophys. Res. Space Phys.* 122, 9068–9079. doi:10.1002/2016JA023342

Klein, K. G., Spence, H., Alexandrova, O., Argall, M., Arzamasskiy, L., Bookbinder, J., et al. (2023). Helioswarm: a multipoint, multiscale mission to characterize turbulence. *Space Sci. Rev.* 219, 74. doi:10.1007/s11214-023-01019-0

Kozyreva, O., Pilipenko, V., Lorentzen, D., Baddeley, L., and Hartinger, M. (2019). Transient oscillations near the dayside open-closed boundary: evidence of magnetopause surface mode? *J. Geophys. Res. Space Phys.* 124, 9058–9074. doi:10.1029/2018JA025684

Kozyreva, O. V., Pilipenko, V. A., Bland, E. C., Baddeley, L. J., and Zakharov, V. I. (2020). Periodic modulation of the upper ionosphere by ULF waves as observed simultaneously by superdarn radars and gps/tec technique. *J. Geophys. Res. Space Phys.* 125, e2020JA028032. doi:10.1029/2020JA028032

Liang, J., Donovan, E., Jackel, B., Spanswick, E., and Gillies, M. (2016). On the 630 nm red-line pulsating aurora: red-line Emission Geospace Observatory observations and model simulations. *J. Geophys. Res. Space Phys.* 121, 7988–8012. doi:10.1002/2016JA022901

Liang, J., Gillies, D., Donovan, E., Parry, H., Mann, I., Connors, M., et al. (2022). On the green isolated proton auroras during Canada thanksgiving geomagnetic storm. *Front. Astron. Space Sci.* 9, 1040092. doi:10.3389/fspas.2022.1040092

Liang, J., Gillies, D. M., Spanswick, E., and Donovan, E. F. (2024). Converting TREx-RGB green-channel data to 557.7 nm auroral intensity: methodology and initial results. *Earth Planet. Phys.* 8, 258–274. doi:10.26464/epp2023063

Lin, D., Wang, C., Li, W., Tang, B., Guo, X., and Peng, Z. (2014). Properties of Kelvin-Helmholtz waves at the magnetopause under northward interplanetary magnetic field: statistical study. *J. Geophys. Res. Space Phys.* 119, 7485–7494. doi:10.1002/2014JA020379

Liou, K., Takahashi, K., Newell, P. T., and Yumoto, K. (2008). Polar ultraviolet imager observations of solar wind-driven ULF auroral pulsations. *Geophys. Res. Lett.* 35, L16101. doi:10.1029/2008GL034953

Lundin, R., and Evans, D. S. (1985). Boundary layer plasmas as a source for high-latitude, early afternoon, auroral arcs. *Planet. Space Sci.* 33, 1389–1406. doi:10.1016/0032-0633(85)90115-1

Lyatsky, W. B., and Sibeck, D. G. (1997). Surface waves on the low-latitude boundary layer inner edge and travelling convection vortices. *J. Geophys. Res. Space Phys.* 102, 17643–17647. doi:10.1029/97JA00323

Ma, X., Delamere, P., Otto, A., and Burkholder, B. (2017). Plasma transport driven by the three-dimensional Kelvin-Helmholtz instability. *J. Geophys. Res. Space Phys.* 122, 10382–10395. doi:10.1002/2017JA024394

Ma, X., Otto, A., and Delamere, P. A. (2014). Interaction of magnetic reconnection and Kelvin-Helmholtz modes for large magnetic shear: 1. Kelvin-Helmholtz trigger. *J. Geophys. Res. Space Phys.* 119, 781–797doi. doi:10.1002/2013JA019224

Masson, A., and Nykyri, K. (2018). Kelvin-Helmholtz instability: lessons learned and ways forward. *Space Sci. Rev.* 214, 71. doi:10.1007/s11214-018-0505-6

Masters, A., Achilleos, N., Bertucci, C., Dougherty, M. K., Kanani, S. J., Arridge, C. S., et al. (2009). Surface waves on Saturn's dawn flank magnetopause driven by the Kelvin–Helmholtz instability. *Planet. Space Sci.* 57, 1769–1778. doi:10.1016/j.pss.2009.02.010

Matlsev, Y. P., and Lyatsky, W. B. (1975). Field-aligned currents and erosion of the dayside magnetosphere. *Planet. Space Sci.* 23, 1257–1260. doi:10.1016/0032-0633(75)90149-X

McWilliams, K. A., Detwiller, M., Kotyk, K., Krieger, K., Rohel, R., Billett, D. D., et al. (2023). Borealis: an advanced digital hardware and software design for superdarn radar systems. *Radio Sci.* 58, e2022RS007591. doi:10.1029/2022RS007591

Mejnertsen, L., Eastwood, J. P., Hietala, H., Schwartz, S. J., and Chittenden, J. P. (2017). Global MHD simulations of the earth's bow shock shape and motion under variable solar wind conditions. *J. Geophys. Res. Space Phys.* 123, 259–271. doi:10.1002/2017JA024690

Mende, S. B., Harris, S. E., Frey, H. U., Angelopoulos, V., Russell, C. T., Donovan, E., et al. (2008). The THEMIS array of ground-based observatories for the study of auroral substorms, *Space Sci. Rev.*, 141, 357–387. doi:10.1007/s11214-008-9380-x

Mende, S. B., Heetderks, H., Frey, H. U., Lampton, M., Geller, S. P., Abiad, R., et al. (2000a). Far ultraviolet imaging from the IMAGE spacecraft. 2. Wideband FUV imaging. *Space Sci. Rev.* 91, 271–285. doi:10.1023/A:1005227915363

Mende, S. B., Heetderks, H., Frey, H. U., Lampton, M., Geller, S. P., Habraken, S., et al. (2000b). Far ultraviolet imaging from the IMAGE spacecraft. 1. System design. *Space Sci. Rev.* 91, 243–270. doi:10.1007/978-94-011-4233-5_8

Mende, S. B., Heetderks, H., Frey, H. U., Stock, J. M., Lampton, M., Geller, S. P., et al. (2000c). "Far ultraviolet imaging from the IMAGE spacecraft. 3. Spectral imaging of lyman- and OI 135.6 nm," in *The IMAGE mission*. Editor J. L. Burch (chap: Springer Netherlands), 287–318. doi:10.1007/978-94-011-4233-5_103

Merkin, V. G., Kondrashov, D., Ghil, M., and Anderson, B. J. (2016). Data assimilation of low-altitude magnetic perturbations into a global magnetosphere model. *Space weather.* 14, 165–184. doi:10.1002/2015SW001330

Milan, S. E., Clausen, L. B. N., Coxon, J. C., Carter, J. A., Walach, M.-T., Laundal, K., et al. (2017). Overview of solar wind–magnetosphere–ionosphere–atmosphere coupling and the generation of magnetospheric currents. *Space Sci. Rev.* 206, 547–573. doi:10.1007/s11214-017-0333-0

Milan, S. E., Sato, N., Ejiri, M., and Moen, J. (2001). Auroral forms and the field-aligned current structure associated with field line resonances. *J. Geophys. Res. Space Phys.* 106, 25825–25833. doi:10.1029/2001JA900077

Montgomery, J., Ebert, R. W., Allegrini, F., Bagenal, F., Bolton, S. J., DiBraccio, G. A., et al. (2023). Investigating the occurrence of Kelvin-Helmholtz instabilities at Jupiter's dawn magnetopause. *Geophys. Res. Lett.* 50, e2023GL102921. doi:10.1029/2023GL102921

Motoba, T., Fujita, S., Kikuchi, T., and Tanaka, T. (2007). Solar wind dynamic pressure forced oscillation of the magnetosphere-ionosphere coupling system: a numerical simulation of directly pressure-forced geomagnetic pulsations. *J. Geophys. Res. Space Phys.* 112, A11204. doi:10.1029/2006JA012193

Murphy, K. R., Inglis, A. R., Sibeck, D. G., Watt, C. E. J., and Rae, I. J. (2020). Inner magnetospheric ULF waves: the occurrence and distribution of broadband and discrete wave activity. *J. Geophys. Res. Space Phys.* 125, e27887. doi:10.1029/2020JA027887

Nakariakov, V. M., Pilipenko, V., Heilig, B., Jelínek, P., Karlický, M., Klimushkin, D. Y., et al. (2016). Magnetohydrodynamic oscillations in the solar corona and Earth's magnetosphere: towards consolidated understanding. *Space Sci. Rev.* 200, 75–203. doi:10.1007/s11214-015-0233-0

Nguyen, G., Aunai, N., de Welle, B. M., Jeandet, A., Lavraud, B., and D, F. (2022). Massive multi-mission statistical study and analytical modeling of the earth's magnetopause: 1. a gradient boosting based automatic detection of near-earth regions. *J. Geophys. Res. Space Phys.* 127, e2021JA029773. doi:10.1029/2021JA029773

Nicolla, M. J., and Heinselman, C. J. (2007). Three-dimensional measurements of traveling ionospheric disturbances with the poker flat incoherent scatter radar. *Geophys. Res. Lett.* 34, L21104. doi:10.1029/2007GL031506

Nishitani, N., Ruohoniemi, J. M., Lester, M., Baker, J. B. H., Koustov, A. V., Shepherd, S. G., et al. (2019). Review of the accomplishments of mid-latitude super dual auroral radar network (superdarn) hf radars. *Prog. Earth Planet. Sci.* 6, 27. doi:10.1186/s40645-019-0270-5

Nykyri, K., Begtson, M., Angelopoulos, V., Nishimura, Y., and Wing, S. (2019). Can enhanced flux loading by high-speed jets lead to a substorm? multipoint detection of the christmas day substorm onset at 08:17 UT, 2015. *J. Geophys. Res. Space Phys.* 124, 4314–4340. doi:10.1029/2018JA026357

Nykyri, K., Johnson, J., Kronberg, E., Turner, D., Wing, S., Cohen, I., et al. (2021). Magnetospheric Multiscale observations of the source region of energetic electron microinjections along the duskside, high-latitude magnetopause boundary layer. *Geophys. Res. Lett.* 48, e2021GL092466. doi:10.1029/2021GL092466

Oliveira, D. M., Hartinger, M. D., Xu, Z., Zesta, E., Pilipenko, V. A., Giles, B. L., et al. (2020). Interplanetary shock impact angles control magnetospheric ULF wave activity: wave amplitude, frequency, and power spectra. *Geophys. Res. Lett.* 47, e90857. doi:10.1029/2020GL090857

Paschmann, G., and Daly, P. W. (1998) "Analysis methods for multi-spacecraft data," in *ISSI scientific reports*. Bern, Switzerland: International Space Science Institute.

Paschmann, G., Haaland, S., Sonnerup, B. U. O., Hasegawa, H., Georgescu, E., Klecker, B., et al. (2005). Characteristics of the near-tail dawn magnetopause and boundary layer. *Ann. Geophys.* 23, 1481–1497. doi:10.5194/angeo-23-1481-2005

Paxton, L. J., Morrison, D., Zhang, Y., Kil, H., Wolven, B., Ogorzalek, B. S., et al. (2002). Validation of remote sensing products produced by the special sensor ultraviolet scanning imager (ssusi): a far uv-imaging spectrograph on dmsp f-16. Optical spectroscopic techniques, remote sensing, and instrumentation for atmospheric and space research IV (SPIE) 4485, 338–348.

Piersanti, M., Materassi, M., Cicone, A., Spogli, L., Zhou, H., and Ezquer, R. G. (2018). Adaptive local iterative filtering: a promising technique for the analysis of nonstationary signals. *J. Geophys. Res. Space Phys.* 123, 1031–1046. doi:10.1002/2017JA024153

Pilipenko, V., Belakhovsky, V., Engebretson, M. J., Kozlovsky, A., and Yeoman, T. (2015). Are dayside long-period pulsations related to the cusp? *Ann. Geophys.* 33, 395–404. doi:10.5194/angeo-33-395-2015

Pilipenko, V., Belakhovsky, V., Murr, D., Fedorov, E., and Engebretson, M. (2014). Modulation of total electron content by ULF Pc5 waves. *J. Geophys. Res. Space Phys.* 119, 4358–4369. doi:10.1002/2013ja019594

Pilipenko, V. A., Kozyreva, O. V., A.Lorentzen, D., and Baddeley, L. J. (2018). The correspondence between dayside long-period geomagnetic pulsations and the open-closed field line boundary. *J. Atmos. Terr. Phys.* 170, 64–74. doi:10.1016/j.jastp.2018.02.012

Plaschke, F., Angelopoulos, V., and Glassmeier, K.-H. (2013). Magnetopause surface waves: THEMIS observations compared to MHD theory. *J. Geophys. Res. Space Phys.* 118, 1483–1499. doi:10.1002/jgra.50147

Plaschke, F., and Glassmeier, K. H. (2011). Properties of standing Kruskal-Schwarzschild-modes at the magnetopause. *Ann. Geophys.* 29, 1793–1807. doi:10.5194/angeo-29-1793-2011

Plaschke, F., Glassmeier, K.-H., Auster, H. U., Angelopoulos, V., Constantinescu, O. D., Fornaçon, K.-H., et al. (2009). Statistical study of the magnetopause motion: first results from THEMIS. *J. Geophys. Res. Space Phys.* 114, A00C10. doi:10.1029/2008JA013423

Potemra, T. A., Lühr, H., Zanetti, L. J., Takahashi, K., Erlandson, R. E., Marklund, G. T., et al. (1989). Multisatellite and ground-based observations of transient ULF waves. *J. Geophys. Res.* 94, 2543–2554. doi:10.1029/JA094iA03p02543

Redmon, R. J., Denig, W. F., Kilcommons, L. M., and Knipp, D. J. (2017). New DMSP database of precipitating auroral electrons and ions. *J. Geophys. Res. Space Phys.* 122, 9056–9067. doi:10.1002/2016JA023339

Retinò, A., Khotyaintsev, Y., Le Contel, O., Marcucci, M. F., Plaschke, F., Vaivads, A., et al. (2022). Particle energization in space plasmas: towards a multi-point, multi-scale plasma observatory. *Exp. Astron.* 54, 427–471. doi:10.1007/s10686-021-09797-7

Rietveld, M. T., Senior, A., Markkanen, J., and Westman, A. (2019). New capabilities of the upgraded EISCAT high-power HF facility. *Radio Sci.* 51, 1533–1546. doi:10.1002/2016RS006093

Robertson, I. P., and Cravens, T. E. (2003). X-ray emission from the terrestrial magnetosheath. *Geophys. Res. Lett.* 30, 1439. doi:10.1029/2002GL016740

Ruohoniemi, J. M., and Greenwald, R. A. (1996). Statistical patterns of high-latitude convection obtained from Goose Bay HF radar observations. *J. Geophys. Res.* 101, 21743–21763. doi:10.1029/96JA01584

Ruohoniemi, J. M., Greenwald, R. A., Baker, K. B., Villain, J.-P., Hanuise, C., and Kelly, J. (1989). Mapping high-latitude plasma convection with coherent HF radars. *J. Geophys. Res.* 94, 13463–13477. doi:10.1029/JA094iA10p13463

Samson, J. C., Cogger, L. L., and Pao, Q. (1996). Observations of field line resonances, auroral arcs, and auroral vortex structures. *J. Geophys. Res. Space Phys.* 101, 17373–17383. doi:10.1029/96JA01086

Samsonov, A., Branduardi-Raymont, G., Sembay, S., Read, A., Sibeck, D., and Rastaetter, L. (2024). Simulation of the SMILE Soft X-ray Imager response to a southward interplanetary magnetic field turning. *Earth Planet. Phys.* 8, 39–46. doi:10.26464/epp2023058

Samsonov, A., Sembay, S., Read, A., Carter, J. A., Branduardi-Raymont, G., Sibeck, D., et al. (2022). Finding magnetopause standoff distance using a Soft X-ray Imager: 2. methods to analyze 2-D X-ray images. *J. Geophys. Res.:Space Phys.* 127, e2022JA030850. doi:10.1029/2022JA030850

Schultz, A. (2010). Emscope: a continental scale magnetotelluric observatory and data discovery resource. *Data Sci. J.* 8, IGY6–IGY20. doi:10.2481/dsj.ss_igy-009

Shi, X., Hartinger, M. D., Baker, J. B. H., Murphy, B. S., Bedrosian, P. A., Kelbert, A., et al. (2022). Characteristics and sources of intense geoelectric fields in the United States: comparative analysis of multiple geomagnetic storms. *Space weather.* 20, e2021SW002967. doi:10.1029/2021SW002967

Shi, X., Hartinger, M. D., Baker, J. B. H., Ruohoniemi, J. M., Lin, D., Xu, Z., et al. (2020). Multipoint conjugate observations of dayside ULF waves during an extended period of radial IMF. *J. Geophys. Res. Space Phys.* 125, e2020JA028364. doi:10.1029/2020ja028364

Shi, X., Lin, D., Wang, W., Baker, J. B. H., Weygand, J. M., Hartinger, M. D., et al. (2022). Geospace concussion: global reversal of ionospheric vertical plasma drift in response to a sudden commencement. *Geophys. Res. Lett.* 49, e2022GL100014. doi:10.1029/2022GL100014

Shi, X., Schmidt, M., Martin, C. J., Billett, D. D., Bland, E., Tholley, F. H., et al. (2022). pydarn: a python software for visualizing superdarn radar data. *Front. Astronomy Space Sci.* 9, 1022690. doi:10.3389/fspas.2022.1022690

Sibeck, D. G. (1990). A model for the transient magnetospheric response to sudden solar wind dynamic pressure variations. *J. Geophys. Res.* 95, 3755–3771. doi:10.1029/JA095iA04p03755

Sibeck, D. G., Allen, R., Aryan, H., Bodewits, D., Brandt, P., Branduardi-Raymont, G., et al. (2018). Imaging plasma density structures in the soft x-rays generated by solar wind charge exchange with neutrals. *Space Sci. Rev.* 214, 79. doi:10.1007/s11214-018-0504-7

Sibeck, D. G., Baumjohann, W., and Lopez, R. E. (1989). Solar wind dynamic pressure variations and transient magnetospheric signatures. *Geophys. Res. Lett.* 16, 13–16. doi:10.1029/GL016i001p00013

Sibeck, D. G., Borodkova, N., Schwartz, S., Owen, C., Kessel, R., Kokubun, S., et al. (1999). Comprehensive study of the magnetospheric response to a hot flow anomaly. *J. Geophys. Res. Space Phys.* 104, 4577–4593. doi:10.1029/1998JA900021

Silverman, B. W. (1986) "Density estimation for statistics and data analysis," in *Monographs on statistics and applied probability*. London, UK: Chapman & Hall.

Smit, G. R. (1968). Oscillatory motion of the nose region of the magnetopause. *J. Geophys. Res.* 73, 4990–4993. doi:10.1029/JA073i015p04990

Sorathia, K. A., Merkin, V. G., Panov, E. V., Zhang, B., Lyon, J. G., Garretson, J., et al. (2020). Ballooning-interchange instability in the near-earth plasma sheet and auroral beads: global magnetospheric modeling at the limit of the MHD approximation: *Geophys. Res. Lett.*, 47, e2020GL088227. doi:10.1029/2020GL088227

Sorathia, K. A., Michael, A., Merkin, V. G., Ohtani, S., Keesee, A. M., Sciola, A., et al. (2023). Multiscale magnetosphere-ionosphere coupling during stormtime: a case study of the dawnside current wedge. *J. Geophys. Res. Space Phys.* 128, e2023JA031594. doi:10.1029/2023JA031594

Stallone, A., Cicone, A., and Materassi, M. (2020). New insights and best practices for the successful use of empirical mode decomposition, iterative filtering and derived algorithms. *Sci. Rep.* 10, 15161. doi:10.1038/s41598-020-72193-2

Stamm, J., Verinen, J., Urco, J. M., Gustavsson, B., and Chau, J. L. (2021). Radar imaging with EISCAT 3D. *Ann. Geophys.* 39, 119–134doi. doi:10.5194/angeo-39-119-2021

Torr, M. R., Torr, D. G., Zukic, M., Johnson, R. B., Ajello, J., Banks, P., et al. (1995). A far ultraviolet imager for the international solar-terrestrial physics mission. *Space Sci. Rev.* 71, 329–383. doi:10.1007/BF00751335

Tsyganenko, N. A. (1995). Modeling the earth's magnetospheric magnetic field confined within a realistic magnetopause. *J. Geophys. Res.* 100, 5599–5612. doi:10.1029/94JA03193

Tsyganenko, N. A., and Sitnov, M. I. (2007). Magnetospheric configurations from a high-resolution data-based magnetic field model. *J. Geophys. Res. Space Phys.* 112, A06225. doi:10.1029/2007JA012260

Viall, N. M., Kepko, L., and Spence, H. E. (2009). Relative occurrence rates and connection of discrete frequency oscillations in the solar wind density and dayside magnetosphere. *J. Geophys. Res. Space Phys.* 114, A01201. doi:10.1029/2008JA013334

Villante, U., Recchiuti, D., and Di Matteo, S. (2022). The transmission of ULF waves from the solar wind to the magnetosphere: an analysis of some critical aspects. *Front. Astronomy Space Sci.* 9, 835539. doi:10.3389/fspas.2022.835539

Walach, M.-T., and Grocott, A. (2019). SuperDARN observations during geomagnetic storms, geomagnetically active times, and enhanced solar wind driving. *J. Geophys. Res. Space Phys.* 124, 5828–5847. doi:10.1029/2019JA026816

Walach, M.-T., Grocott, A., and Milan, S. E. (2021). Average ionospheric electric field morphologies during geomagnetic storm phases. *J. Geophys. Res. Space Phys.* 126, e2020JA028512. doi:10.1029/2020JA028512

Walsh, B. M., Kuntz, K. D., Busk, S., Cameron, T., Chornay, D., Chuchra, A., et al. (2024). The lunar environment heliophysics x-ray imager (lexi) mission. *Space Sci. Rev.* 220, 37. doi:10.1007/s11214-024-01063-4

Walsh, B. M., Thomas, E. G., Hwang, K.-J., Baker, J. B. H., Ruohoniemi, J. M., and Bonnell, J. W. (2015). Dense plasma and kelvin-helmholtz waves at earth's dayside magnetopause. *J. Geophys. Res. Space Phys.* 120, 5560–5573. doi:10.1002/2015JA021014

Wang, B., Liu, T., Nishimura, Y., Zhang, H., Hartinger, M., Shi, X., et al. (2020a). Global propagation of magnetospheric Pc5 ULF waves driven by foreshock transients. *J. Geophys. Res. Space Phys.* 125, e2020JA028411. doi:10.1029/2020JA028411

Wang, B., Nishimura, Y., Hartinger, M., Sivadas, N., Lyons, L. L., Varney, R. H., et al. (2020b). Ionospheric modulation by storm time Pc5 ULF pulsations and the structure detected by pfisr-themis conjunction. *Geophys. Res. Lett.* 47, e2020GL089060. doi:10.1029/2020GL089060

Wang, C., and Branduardi-Raymont, G. (2022). Progress of solar wind magnetosphere ionosphere link explorer (SMILE) mission. *Chin. J. Space Sci.* 38, 657–661. doi:10.11728/cjss2018.05.657

Wang, C., and Sun, T. R. (2022). Methods to derive the magnetopause from soft X-ray images by the SMILE mission. *Geosci. Lett.* 9, 30. doi:10.1186/s40562-022-00240-z

Waters, C. L., Anderson, B. J., Green, D. L., Korth, H., Barnes, R. J., and Vanhamäki, H. (2019). Science data products for AMPERE. *ISSI Sci. Rep. Ser.*, 141–165. doi:10.1007/978-3-030-26732-2_7

Watson, C., Jayachandran, P., Singer, H. J., Redmon, R. J., and Danskin, D. (2015). Large-amplitude gps tec variations associated with pc5–6 magnetic field variations observed on the ground and at geosynchronous orbit. *J. Geophys. Res. Space Phys.* 120, 7798–7821. doi:10.1002/2015ja021517

Watson, C., Jayachandran, P. T., and MacDougall, J. W. (2016). Characteristics of gps tec variations in the polar cap ionosphere. *J. Geophys. Res. Space Phys.* 121, 4748–4768. doi:10.1002/2015JA022275

Weygand, J. M., Hartinger, M. D., Strangeway, R. J., Welling, D. T., Kim, H., Matzka, J., et al. (2023). Interhemispheric asymmetry due to IMF by within the cusp spherical elementary currents. *J. Geophys. Res. Space Phys.* 128, e2023JA031430. doi:10.1029/2023JA031430

Yau, A. W., and James, H. G. (2015). Cassiope enhanced polar outflow probe (e-POP) mission overview. *Space Sci. Rev.* 189, 3–14. doi:10.1007/s11214-015-0135-1

Yizengaw, E., Zesta, E., Moldwin, M. B., Magoun, M., Tripathi, N. K., Surussavadee, C., et al. (2018). ULF wave-associated density irregularities and scintillation at the equator. *Geophys. Res. Lett.* 45, 5290–5298. doi:10.1029/2018GL078163

Zhang, B., Sorathia, K. A., Lyon, J. G., Merkin, V. G., Garretson, J. S., and Wiltberger, M. (2019). GAMERA: a three-dimensional finite-volume MHD solver for non-orthogonal curvilinear geometries. *Astrophysical J. Suppl. Ser.* 244, 20. doi:10.3847/1538-4365/ab3a4c